Lynch TJ, Bell DW, Sordella R, Gurubhagavatula S, Okimoto RA, Brannigan BW *et al.* (2004). Activating mutations in the epidermal growth factor receptor underlying responsiveness of non-small-cell lung cancer to gefitinib. *N Engl J Med* **350**: 2129 2139.

Ma PC, Jagadeeswaran R, Jagadeesh S, Tretiakova MS, Nallasura V, Fox EA *et al.* (2005a). Functional expression and mutations of c-Met and its therapeutic inhibition with SU11274 and small interfering RNA in non-small cell lung cancer. *Cancer Res* **65**: 1479 1488.

Ma PC, Kijima T, Maulik G, Fox EA, Sattler M, Griffin JD *et al.* (2003a). c-MET mutational analysis in small cell lung cancer: novel juxtamembrane domain mutations regulating cytoskeletal functions. *Cancer Res* **63**: 6272 6281.

Ma PC, Maulik G, Christensen J, Salgia R. (2003b). c-Met: structure, functions and potential for therapeutic inhibition. *Cancer Metastasis Rev* **22**: 309 325.

Ma PC, Schaefer E, Christensen JG, Salgia R. (2005b). A selective small molecule c-MET Inhibitor, PHA665752, cooperates with rapamycin. *Clin Cancer Res* **11**: 2312 2319.

Ma PC, Tretiakova MS, Nallasura V, Jagadeeswaran R, Husain AN, Salgia R. (2007). Downstream signalling and specific inhibition of c-MET/HGF pathway in small cell lung cancer: implications for tumour invasion. *Br J Cancer* **97**: 368 377.

Mazzone M, Comoglio PM. (2006). The Met pathway: master switch and drug target in cancer progression. *FASEB J* **20**: 1611 1621.

Paez JG, Janne PA, Lee JC, Tracy S, Greulich H, Gabriel S *et al.* (2004). EGFR mutations in lung cancer: correlation with clinical response to gefitinib therapy. *Science* **304**: 1497 1500.

Peruzzi B, Bottaro DP. (2006). Targeting the c-Met signaling pathway in cancer. *Clin Cancer Res* **12**: 3657 3660.

Pevarello P, Brasca MG, Amici R, Orsini P, Traquandi G, Corti L *et al.* (2004). 3-Aminopyrazole inhibitors of CDK2/cyclin A as antitumor agents. 1. Lead finding. *J Med Chem* **47**: 3367 3380.

Rikova K, Guo A, Zeng Q, Possemato A, Yu J, Haack H *et al.* (2007). Global survey of phosphotyrosine signaling identifies oncogenic kinases in lung cancer. *Cell* **131**: 1190 1203.

Scapin G, Patel SB, Lisnock J, Becker JW, LoGrasso PV. (2003). The structure of JNK3 in complex with small molecule inhibitors: structural basis for potency and selectivity. *Chem Biol* **10**: 705 712.

Shigematsu H, Gazdar AF. (2006). Somatic mutations of epidermal growth factor receptor signaling pathway in lung cancers. *Int J Cancer* **118**: 257 262.

Shinomiya N, Gao CF, Xie Q, Gustafson M, Waters DJ, Zhang YW *et al.* (2004). RNA interference reveals that ligand-independent met activity is required for tumor cell signaling and survival. *Cancer Res* **64**: 7962 7970.

Smolen GA, Sordella R, Muir B, Mohapatra G, Barmettler A, Archibald H *et al.* (2006). Amplification of MET may identify a subset of cancers with extreme sensitivity to the selective tyrosine kinase inhibitor PHA-665752. *Proc Natl Acad Sci USA* **103**: 2316 2321.

Stamos J, Sliwkowski MX, Eigenbrot C. (2002). Structure of the epidermal growth factor receptor kinase domain alone and in complex with a 4-anilinoquinazoline inhibitor. *J Biol Chem* **277**: 46265 46272.

Tam IY, Chung LP, Suen WS, Wang E, Wong MC, Ho KK *et al.* (2006). Distinct epidermal growth factor receptor and KRAS mutation patterns in non-small cell lung cancer patients with different tobacco exposure and clinicopathologic features. *Clin Cancer Res* **12**: 1647 1653.

Tang Z, Du R, Jiang S, Wu C, Barkauskas DS, Richey J *et al.* (2008). Dual MET-EGFR combinatorial inhibition against T790M-EGFR-mediated erlotinib-resistant lung cancer. *Br J Cancer* **99**: 911 922, 2008.

Thomas RK, Baker AC, Debiasi RM, Winckler W, Laframboise T, Lin WM *et al.* (2007). High-throughput oncogene mutation profiling in human cancer. *Nat Genet* **39**: 347 351.

Wood ER, Truesdale AT, McDonald OB, Yuan D, Hassell A, Dickerson SH *et al.* (2004). A unique structure for epidermal growth factor receptor bound to GW572016 (Lapatinib): relationships among protein conformation, inhibitor off-rate, and receptor activity in tumor cells. *Cancer Res* **64**: 6652 6659.

Zhang X, Gureasko J, Shen K, Cole PA, Kuriyan J. (2006). An allosteric mechanism for activation of the kinase domain of epidermal growth factor receptor. *Cell* **125**: 1137 1149.

Zhu X, Kim JL, Newcomb JR, Rose PE, Stover DR, Toledo LM *et al.* (1999). Structural analysis of the lymphocyte-specific kinase Lck in complex with non-selective and Src family selective kinase inhibitors. *Structure* **7**: 651 661.

Supplementary Information accompanies the paper on the Oncogene website (http://www.nature.com/onc)

Pathology International 2008; **58**: 253–256 doi:10.1111/j.1440-1827.2008.02220.x

Short Communication

Pleural MALT lymphoma diagnosed on thoracoscopic resection under local anesthesia using an insulation-tipped diathermic knife

Kunimitsu Kawahara,[1] Shinji Sasada,[2] Teruaki Nagano,[1] Hidekazu Suzuki,[2] Masashi Kobayashi,[2] Kaoru Matsui,[2] Katsuyoshi Takata,[3] Tadashi Yoshino,[3] Tomoki Michida[4] and Teruo Iwasaki[5]

Departments of [1]Pathology, [2]Thoracic Malignancy and [5]Respiratory Surgery, Osaka Prefectural Medical Center for Respiratory and Allergic Diseases, Habikino, [3]Department of Pathology, Okayama University Graduate School of Medicine, Dentistry and Pharmaceutical Sciences, Okayama and [4]Department of Internal Medicine, Osaka Koseinenkin Hospital, Osaka, Japan

A 79-year-old man presented with back pain. Chest CT scan showed elevated nodular lesions in the right parietal pleurae with pleural effusion. There were no intrapulmonary or mediastinal abnormalities. Under local anesthesia, right thoracoscopy and subsequent thoracoscopic pleural resection were performed using an insulation-tipped diathermic knife (IT-knife). The resected pleura, 2.2 cm in diameter, had a rough granular surface. Lymphoid cells histologically infiltrated diffusely into the pleura. They were composed of centrocyte-like and monocytoid cells. On immunohistochemistry they were found to be positive for Bcl2, CD20, CD45RB and CD79a, but negative for CD3, CD5, CD10 and cyclin D1. EBV-encoded small RNA-1 (EBER-1) *in situ* hybridization was negative. A diagnosis of extranodal marginal zone B-cell lymphoma of mucosa-associated lymphoid tissue (MALT lymphoma) arising in the pleura was therefore made. To the authors' knowledge this is the first case in which IT-knife was used for diagnosis of a pleural lesion. This large, single-piece, only slightly crushed pleural specimen, enabled study of histopathological findings (listed here) that could not have been obtained on conventional biopsy: (i) lack of apparent evidence of plasmacytic differentiation; (ii) no recognition of lymphoid follicles; (iii) mesothelial cells not infiltrated by lymphoma cell clusters; (iv) thin layer of hyperplastic mesothelial cells continuously covering the surface; and (v) no proliferation of fibroblast-like submesothelial cells.

Key words: insulation-tipped diathermic knife, MALT lymphoma, pleura, thoracoscopy

Correspondence: Kunimitsu Kawahara, MD, PhD, Department of Pathology, Osaka Prefectural Medical Center for Respiratory and Allergic Diseases, 3-7-1 Habikino, Habikino-shi, Osaka 583-8588, Japan. Email: kawahara@hbk.pref.osaka.jp

Received 18 August 2007. Accepted for publication 20 November 2007.

Extranodal marginal zone B-cell lymphoma of mucosa-associated lymphoid tissue (MALT lymphoma) arising in the pleura is extremely rare, with only four published cases.[1–3] Reported cases were diagnosed pathologically using surgically resected pleural specimen under thoracotomy[1,3] or under video-assisted thoracic surgery (VATS).[2] But in these cases the histopathological findings were not described in detail, probably because the obtained specimens were fragmented or highly crushed. To resolve these issues, large, single-piece and only slightly crushed resected specimens are necessary.

In Japan, endoscopic mucosal resection (EMR) of gastric mucosa by gastrointestinal endoscopists has been accepted as a treatment option for early gastric cancer (EGC).[4] For resection of larger EGC as a single-piece specimen, a new EMR method using an insulation-tipped diathermic knife (IT-knife; Olympus, Tokyo, Japan) was developed.[4–6]

Herein we present the first case of pleural MALT lymphoma that was diagnosed thoracoscopically using a large and single-piece specimen obtained using an IT-knife (thoracoscopic IT-knife) and describe the histopathological findings of pleural MALT lymphoma in detail.

CASE REPORT

Clinical history

A 79-year-old man who had smoked approximately 60 cigarettes per day for 40 years, consulted Osaka Prefectural Medical Center for Respiratory and Allergic Diseases complaining of back pain that had persisted for 2 months. Family

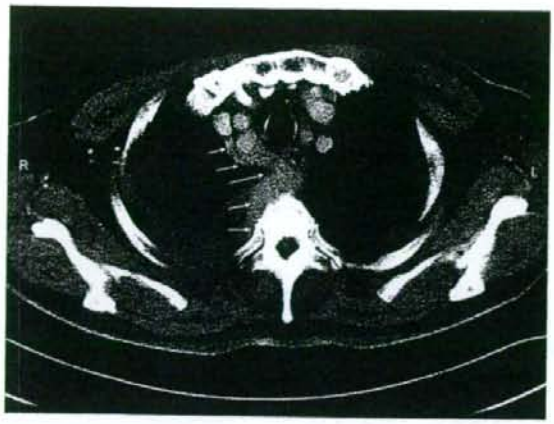

Figure 1 Chest CT scan showing diffuse prominent thickening of right mediastinal pleura (arrows) and pleural effusion.

history, past medical history and occupational history were unremarkable. Chest CT scan (Fig. 1) showed diffuse prominent thickening of the right mediastinal and costal pleurae. Right pleural effusion was present but there were no intrapulmonary or mediastinal abnormalities. Pleural effusion cytology did not show any evidence of neoplasia. Laboratory tests and CT scan of the abdomen and pelvis were unremarkable. Serum CEA, neuron-specific enolase, cytokeratin-19 fragment and soluble interleukin-2-receptor levels were 4.7 ng/mL (cut-off: 5 ng/mL) , 10.4 ng/mL (cut-off: 10 ng/mL), 1.3 ng/mL (cut-off: 3.5 ng/mL) and 857 U/mL (cut-off: 466 U/mL), respectively. A tentative diagnosis of pleural malignant mesothelioma was made. After removal of 1340 mL of pleural effusion, a thoracoscopic IT-knife was used to resect a nodular lesion in the costal parietal pleura under local anesthesia (Fig. 2a,b).

Macroscopic findings

The resected pleura measured 2.2 cm in diameter and had a rough granular surface (Fig. 2c). The specimen was serially examined at 4 mm intervals. The cut surface (Fig. 2d) was whitish and exhibited prominent thickening of the pleura.

Microscopic findings

Throughout the whole pleural specimen, from the superficial submesothelial layer to the deep margin, a diffuse infiltrate of small- to -medium lymphoid cells was recognized (Fig. 3a). These cells were composed of centrocyte-like and monocytoid cells (Fig. 3b). Plasmacytic differentiation was inconspicuous and lymphoid follicles were absent (Fig. 3b).

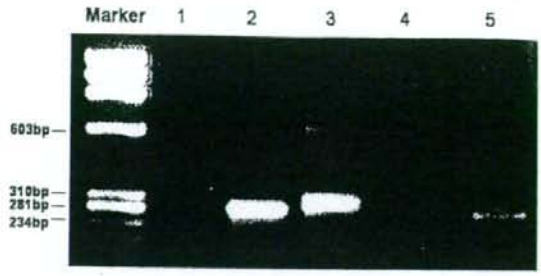

Figure 4 Clonal polymerase chain reaction (PCR). Clonal analysis of immunoglobulin heavy-chain (*IgH*) gene rearrangements was performed using semi-nested PCR. Lane 1, negative control; lane 2, positive control; lane 3, reactive lymphoid hyperplasia; lane 4, present case; lane 5, present case. Two samples (lanes 4, 5) taken from the right costal pleurae had a distinct single clonal band in the PCR assay for the *IgH* gene.

Mitoses were present in 3 figures/50 high-power fields. There was no necrosis or hemorrhage. Immunohistochemistry showed that these cells were positive for Bcl2, CD20, CD45RB and CD79a (Fig. 3c), but negative for CD3, CD5, CD10 and cyclin D1. EBV-encoded small RNA-1 (EBER-1) *in situ* hybridization was negative. Therefore, we made a final diagnosis of pleural MALT lymphoma. AE1/AE3 staining showed that the pleural lesions were covered with a thin continuous layer of hyperplastic mesothelial cells (Fig. 3d), but there was no infiltration of lymphoma cell clusters among the mesothelial cells, like the lymphoepithelial lesions typically seen in gastric lesions (Fig. 3e). There was no proliferation of submesothelial fibroblast-like cells (Fig. 3e).

Clonal analysis by polymerase chain reaction

Clonality analysis of immunoglobulin heavy-chain (*IgH*) gene rearrangements was performed using semi-nested polymerase chain reaction (PCR). The PCR conditions and the primers used (FR2A, LJH and VLJH) have been described previously.[7,8] This case had a distinct single clonal band in the PCR assay for the *IgH* gene (Fig. 4).

DISCUSSION

MALT lymphoma is an extranodal indolent lymphoma consisting of morphologically heterogenous small B-cells: marginal zone (centrocyte-like) cells, monocytoid cells, small lymphocytes, and scattered immunoblasts and centroblast-like cells.[9] The gastrointestinal tract is the most common site.[9] In the present case a diffuse infiltrate of small- to -medium lymphoid cells was recognized in the pleural specimens. Plasmacytic differentiation was inconspicuous and

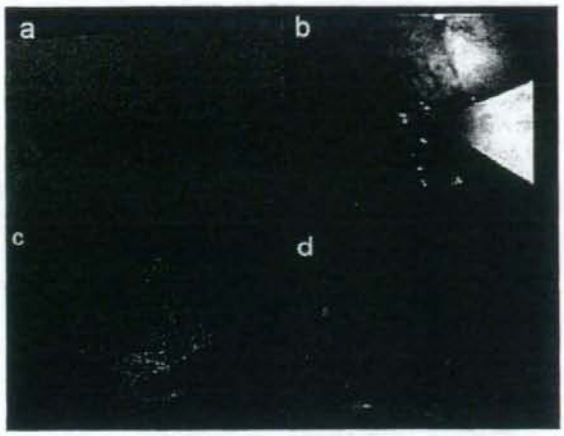

Figure 2 (**a**) Insulated-tipped diathermic knife (IT-knife): Needle knife with a ceramic ball at the top. (**b**) Thoracoscopic image showing a nodular lesion in the parietal pleura being incised. (**c**) Resected pleura with a rough granular surface. Bar, 1 cm (**d**) Cut surface showing prominent thickening of the pleura and a whitish appearance. Bar, 1 cm.

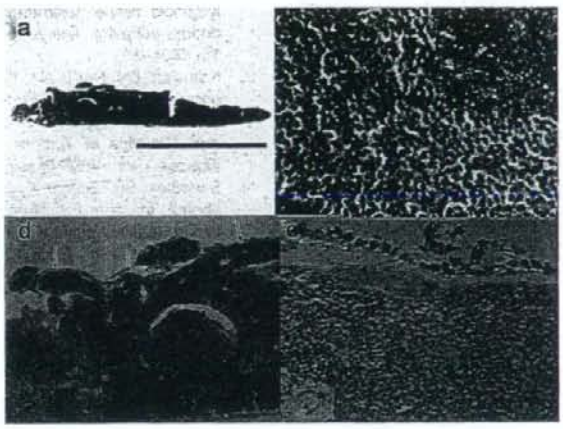

Figure 3 (**a**) Diffuse infiltrate of lymphoid cells through all layers of the pleura. Bar, 1 cm (**b**) Tumor cells composed of centrocyte-like and monocytoid lymphoid cells without apparent plasmacytic differentiation or follicular formation. (**c**) CD79a staining showing positivity for most tumor cells. (**d**) AE1/AE3 staining: thin layer of hyperplastic mesothelial cells (arrows). These cells covered the surfaces of pleural granular lesions. (**e**) AE1/AE3 staining did not show any proliferation of submesothelial fibroblast-like cells.

lymphoid follicles were completely absent histologically. These microscopic features also indicated another possibility of mature B-cell neoplasms including follicular lymphoma and mantle cell lymphoma. Most cases of follicular lymphoma are composed of small to medium-sized cells (centrocytes) and large transformed cells (centroblasts).[10] Large cell components were absent in the present case. Immunohistochemically, these tumor cells of follicular lymphoma are usually positive for CD10,[10] but this was negative in the present case. The neoplastic cells of mantle cell lymphoma are composed of small to medium-sized lymphoid cells most closely resembling centrocytes.[11] They are typically CD5 and cyclin D1 positive,[11] but in the present case these two markers were negative.

Until recently, MALT lymphoma primarily involving the pleura had not been documented, until Ahmad *et al.*[2] reported the first two cases of pleural MALT lymphoma; an additional two cases were reported thereafter.[1,3] Of four

cases, pathological diagnosis was made using a biopsy specimen obtained on VATS in two cases.[2] In the remaining two cases, decortication[1] or complete *en bloc* resection[3] was performed under thoracotomy.

In Japan, EMR for gastric mucosa has been accepted as a treatment option for EGC where the probability of lymph node metastasis is low.[4] The specimen obtained on EMR as a single specimen is available for accurate histopathological determination of the submucosal invasion, vessel involvement and marginal invasion. For EMR for a larger EGC, the IT-knife was developed.[4–6] The IT-knife can dissect the gastric submucosa safely, and completely remove a carcinoma as a large single-piece specimen without severe crushing. The use of the IT-knife during thoracoscopic examinations has not previously been reported anywhere. Using this procedure we first obtained a large, single-piece, full-thickness and only slightly crushed specimen of the pleura and were able to study its histopathological features in detail. Previously such thoracoscopic study has been impossible because thoracoscopic biopsy specimens were tiny or crushed by the biopsy forceps.

Beyond expectation, the thoracoscopic IT-knife allowed detailed histopathological findings of pleural MALT lymphoma to be obtained. New histopathological findings for pleural MALT lymphoma are as follows: (i) lack of apparent evidence of plasmacytic differentiation; (ii) no recognition of lymphoid follicles; (iii) mesothelial cells not infiltrated by lymphoma cell clusters; (iv) thin layer of hyperplastic mesothelial cells continuously covering the surfaces; and (v) no proliferation of fibroblast-like submesothelial cells. This new thoracoscopic IT-knife is very useful for the detailed pathological study of pleural lesions including MALT lymphoma.

REFERENCES

1 Mitchell A, Meunier C, Ouellette D, Colby T. Extranodal marginal zone lymphoma of mucosa-associated lymphoid tissue with initial presentation in the pleura. *Chest* 2006; **129**: 791–4.

2 Ahmad H, Pawade J, Falk S, Morgan JA, Balacumaraswami L. Primary pleural lymphomas. *Thorax* 2003; **58**: 908–9.

3 Hirai S, Hamanaka Y, Mitsui N, Morifuji K, Sutoh M. Primary malignant lymphoma arising in the pleura without preceding long-standing pyothorax. *Ann Thorac Cardiovasc Surg* 2004; **10**: 297–300.

4 Ono H, Kondo H, Gotoda T *et al.* Endoscopic mucosal resection for treatment of early gastric cancer. *Gut* 2001; **48**: 225–9.

5 Ohkuwa M, Hosokawa K, Boku N, Ohtu A, Tajiri H, Yoshida S. New endoscopic treatment for intramucosal gastric tumors using an insulated-tip diathermic knife. *Endoscopy* 2001; **33**: 221–6.

6 Miyamoto S, Muto M, Hamamoto Y *et al.* A new technique for endoscopic mucosal resection with an insulated-tip electrosurgical knife improves the completeness of resection of intramucosal gastric neoplasms. *Gastrointest Endosc* 2002; **55**: 576–81.

7 Sato Y, Nakamura N, Nakamura S *et al.* Deviated VH4 immunoglobulin gene usage is found among thyroid mucosa-associated lymphoid tissue lymphomas, similar to the usage at other sites, but is not found in thyroid diffuse large B-cell lymphomas. *Mod Pathol* 2006; **19**: 1578–84.

8 Mannami T, Yoshino T, Oshima K *et al.* Clinical, histopathological, and immunogenetic analysis of ocular adnexal lymphoproliferative disorders: Characterization of malt lymphoma and reactive lymphoid hyperplasia. *Mod Pathol* 2001; **14**: 641–9.

9 Thieblemont C, Bastion Y, Berger F *et al.* Mucosa-associated lymphoid tissue gastrointestinal and nongastrointestinal lymphoma behavior: Analysis of 108 patients. *J Clin Oncol* 1997; **15**: 1624–30.

10 Nathwani BN, Harris NL, Weisenburger D *et al.* Follicular lymphoma. In: Jaffe ES, Harris NL, Stein H, Vardiman JW, eds. *World Health Organization Classifications of Tumors. Pathology and Genetics of Tumors of Haematopoietic and Lymphoid Tissues.* Lyon: IARC Press, 2001; 162–7.

11 Swerdlow SH, Berger F, Isaacson PI *et al.* Mantle cell lymphoma. In: Jaffe ES, Harris NL, Stein H, Vardiman JW, eds. *World Health Organization Classifications of Tumors. Pathology and Genetics of Tumors of Haematopoietic and Lymphoid Tissues.* Lyon: IARC Press, 2001; 168–70.

British Journal of Cancer (2008) 98, 693–696

www.bjcancer.com

Short Communication

Randomised phase II trial of irinotecan plus cisplatin *vs* irinotecan, cisplatin plus etoposide repeated every 3 weeks in patients with extensive-disease small-cell lung cancer

I Sekine*,[1], H Nokihara[1], K Takeda[2], Y Nishiwaki[3], K Nakagawa[4], H Isobe[5], K Mori[6], K Matsui[7], N Saijo[3] and T Tamura[1]

[1]Division of Internal Medicine and Thoracic Oncology, National Cancer Center Hospital, Tokyo, Japan; [2]Department of Clinical Oncology, Osaka City General Hospital, Osaka, Japan; [3]Division of Thoracic Oncology, National Cancer Center Hospital East, Kashiwa, Japan; [4]Department of Medical Oncology, Kinki University School of Medicine, Sayama, Japan; [5]Department of Pulmonary Disease, National Hospital Organization Hokkaido Cancer Center, Sapporo, Japan; [6]Department of Thoracic Diseases, Tochigi Prefectural Cancer Center, Utsunomiya, Japan; [7]Department of Internal Medicine, Osaka Prefectural Medical Center for Respiratory and Allergic Diseases, Habikino, Japan

Patients with previously untreated extensive-disease small-cell lung cancer were treated with irinotecan 60 mg m^{-2} on days 1 and 8 and cisplatin 60 mg m^{-2} on day 1 with ($n = 55$) or without ($n = 54$) etoposide 50 mg m^{-2} on days 1–3 with granulocyte colony-stimulating factor support repeated every 3 weeks for four cycles. The triplet regimen was too toxic to be considered for further studies.

British Journal of Cancer (2008) **98,** 693–696. doi:10.1038/sj.bjc.6604233 www.bjcancer.com
Published online 5 February 2008

Keywords: small-cell lung cancer; chemotherapy; irinotecan; etoposide; three drug combination

Clinical Studies

Small-cell lung cancer (SCLC), which accounts for approximately 14% of all malignant pulmonary tumours, is an aggressive malignancy with a propensity for rapid growth and early widespread metastases (Jackman and Johnson, 2005). A combination of cisplatin and etoposide (PE) has been the standard treatment, with response rates ranging from 60 to 90% and median survival times (MSTs) from 8 to 11 months in patients with extensive disease (ED)-SCLC (Fukuoka *et al*, 1991; Roth *et al*, 1992). A combination of irinotecan and cisplatin (IP) showed a significant survival benefit over the PE regimen (MST: 12.8 *vs* 9.4 months, $P = 0.002$) in a Japanese phase III trial for ED-SCLC (Noda *et al*, 2002), although another phase III trial comparing these regimens failed to show such a benefit (Hanna *et al*, 2006). Thus, irinotecan, cisplatin and etoposide are the current key agents in the treatment of SCLC. A phase II trial of the three agents, IPE combination, in patients with ED-SCLC showed a promising antitumour activity with a response rate of 77%, complete response (CR) rate of 17% and MST of 12.9 months (Sekine *et al*, 2003).

We have developed these IP and IPE regimens in a 4-week schedule where irinotecan was given on days 1, 8 and 15. The dose of irinotecan on day 15, however, was frequently omitted because of toxicity in both regimens (Noda *et al*, 2002; Sekine *et al*, 2003). The objectives of this study were to evaluate the toxicities and antitumour effects of IP and IPE regimens in the 3-week schedule in patients with ED-SCLC and to select the right arm for subsequent phase III trials.

*Correspondence: Dr I Sekine, Division of Internal Medicine and Thoracic Oncology, National Cancer Center Hospital, Tsukiji 5-1-1, Chuo-ku, Tokyo 104-0045, Japan; E-mail: isekine@ncc.go.jp
Received 15 October 2007; revised 2 January 2008; accepted 9 January 2008; published online 5 February 2008

PATIENTS AND METHODS

Patient selection

Patients were enrolled in this study if they met the following criteria: (1) a histological or cytological diagnosis of SCLC; (2) no prior treatment; (3) measurable disease; (4) ED, defined as having distant metastasis or contralateral hilar lymph node metastasis; (5) performance status of 0–2 on the Eastern Cooperative Oncology Group (ECOG) scale; (6) predicted life expectancy of 3 months or longer; (7) age between 20 and 70 years; (8) adequate organ function as documented by a white blood cell (WBC) count $\geqslant 4.0 \times 10^3\,\mu l^{-1}$, neutrophil count $\geqslant 2.0 \times 10^3\,\mu l^{-1}$, haemoglobin $\geqslant 9.5\,g\,dl^{-1}$, platelet count $\geqslant 100 \times 10^3\,\mu l^{-1}$, total serum bilirubin $\leqslant 1.5\,mg\,dl^{-1}$, hepatic transaminases $\leqslant 100\,IU\,l^{-1}$, serum creatinine $\leqslant 1.2\,mg\,dl^{-1}$, creatinine clearance $\geqslant 60\,ml\,min^{-1}$, and $PaO_2 \geqslant 60$ torr; and (9) providing written informed consent.

Patients were not eligible for the study if they had any of the following: (1) uncontrollable pleural, pericardial effusion or ascites; (2) symptomatic brain metastasis; (3) active infection; (4) contraindications for the use of irinotecan, including diarrhoea, ileus, interstitial pneumonitis and lung fibrosis; (5) synchronous active malignancies; (6) serious concomitant medical

illness, including severe heart disease, uncontrollable diabetes mellitus or hypertension; or (7) pregnancy or breast feeding.

Treatment schedule

In the IP arm, cisplatin, 60 mg m^{-2}, was administered intravenously over 60 min on day 1 and irinotecan, 60 mg m^{-2}, was administered intravenously over 90 min on days 1 and 8. Prophylactic granulocyte colony-stimulating factor (G-CSF) was not administered in this arm. In the IPE arm, cisplatin and irinotecan were administered at the same dose and schedule as the IP arm. In addition, etoposide, 50 mg m^{-2}, was administered intravenously over 60 min on days 1–3. Filgrastim 50 μg m^{-2} or lenograstim 2 μg kg^{-1} was subcutaneously injected prophylactically from day 5 to the day when the WBC count exceeded 10.0×10^3 μl^{-1}. Hydration (2500 ml) and a $5HT_3$ antagonist were given on day 1, followed by an additional infusion if indicated in both arms. These treatments were repeated every 3 weeks for a total of four cycles.

Toxicity assessment, treatment modification and response evaluation

Toxicity was graded according to the NCI Common Toxicity Criteria version 2.0.

Doses of anticancer agents in the following cycles were modified according to toxicity in the same manner in both arms. Objective tumour response was evaluated according to the Response Evaluation Criteria in Solid Tumors (RECIST) (Therasse *et al*, 2000).

Study design, data management and statistical considerations

This study was designed as a multi-institutional, prospective randomised phase II trial. This study was registered on 6 September 2005 in the University hospital Medical Information Network (UMIN) Clinical Trials Registry in Japan (http://www.umin.ac.jp/ctr/index.htm), which is acceptable to the International Committee of Medical Journal Editors (ICMJE) (http://www.icmje.org/faq.pdf). The protocol and consent form were approved by the Institutional Review Board of each institution. Patient registration and randomisation were conducted at the Registration Center. No stratification for randomisation was performed in this study. The sample size was calculated according to the selection design for pilot studies based on survival (Liu *et al*, 1993). Assuming that (1) the survival curve was exponential for survivals; (2) the MST of the worse arm was 12 months and that of the better arm was 12 months $\times$ 1.4; (3) the correct selection probability was 90%; and (4) additional follow-up in years after the end of accrual was 1 year, the estimated required number of patients was 51 for each arm. Accordingly, 55 patients for each arm and their accrual period of 24 months were planned for this study.

The dose intensity of each drug was calculated for each patient using the following formula as previously described:

$$\text{The dose intensity (mg m}^{-2}\text{ week}^{-1}\text{)} = \frac{\text{Total milligrams of a drug in all cycles per body surface area}}{\text{Total days of therapy}/7}$$

where total days of therapy is the number of days from day 1 of cycle 1 to day 1 of the last cycle plus 21 days for both arms (Hryniuk and Goodyear, 1990).

Differences in the reason for termination of the treatment and the frequencies of grade 3–4 toxicities were assessed by χ tests. Survival was measured as the date of randomisation to the date of death from any cause or the date of the most recent follow-up for overall survival and to the date of disease progression or the date of death for progression-free survival (PFS). The survival of the arms was estimated by the Kaplan–Meier method and compared in an exploratory manner with log-rank tests (Armitage *et al*, 2002).

RESULTS

Patient characteristics

From March 2003 to May 2005, 55 patients were randomised to IP and 55 patients to IPE. One patient in the IP arm was excluded because the patient was ineligible and did not receive the study treatment. The remaining 109 patients were included in the analyses of toxicity, tumour response and patient survival. There were no differences between the two arms in any demographic characteristics listed (Table 1).

Treatment delivery

Treatment was well tolerated with respect to the number of cycles delivered in both arms (Table 2). Among reasons for termination of the treatment, disease progression was noted in nine (17%)

Table 1 Patient characteristics

	IP ($n=54$)	IPE ($n=55$)
Sex		
Female	11	8
Male	43	47
Age (years)		
Median (range)	63 (42–70)	62 (48–70)
PS		
0	11	12
1	42	41
2	1	2
Weight loss		
0–4%	38	43
5–9%	10	10
⩾10%	6	2

Table 2 Treatment delivery

	IP ($n=54$) No. (%)	IPE ($n=55$) No. (%)
Number of cycles delivered		
6*	—	1 (2)
4	41 (76)	36 (65)
3	6 (11)	6 (11)
2	3 (6)	6 (11)
1	4 (7)	6 (11)
Reasons for termination of the treatment†		
Completion	40 (74)	35 (64)
Disease progression	9 (17)	2 (4)
Toxicity	3 (6)	13 (24)
Patient refusal	2 (4)	4 (7)
Others	0 (0)	1 (2)
Total number of cycles delivered	192 (100)	186 (100)
Total number of omission on day 8	35 (18)	37 (17)
Total number of cycles with dose reduction	28 (15)	31 (17)

†$P=0.013$ by χ^2 test. *Protocol violation.

patients in the IP arm and in two (4%) patients in the IPE arm, whereas toxicity was noted in three (6%) patients in the IP arm and 13 (24%) patients in the IPE arm ($P=0.013$) (Table 2). The dose of irinotecan on day 8 was omitted in 35 (18%) cycles in the IP arm and 37 (17%) cycles in the IPE arm (Table 2). The total dose and dose intensity of cisplatin and etoposide were similar between the IP and IPE arms in the present study (Table 3).

Toxicity

The myelotoxicity was more severe in the IPE arm (Table 4). Grade 3 febrile neutropaenia was noted in 5 (9%) patients in the IP arm and 17 (31%) patients in the IPE arm ($P=0.005$). Packed red blood cells were transfused in 4 (7%) patients in the IP regimen and 14 (26%) patients in the IPE regimen ($P=0.011$). Platelet concentrates were needed in none in the IP regimen and 2 (4%) patients in the IPE regimen ($P=0.16$). Grade 3–4 diarrhoea was observed in 8 (15%) patients in the IP arm and 13 (24%) patients in the IPE arm ($P=0.262$). Grade 3–4 fatigue was more common in the IPE arm with marginal significance (2 *vs* 11%, $P=0.054$). The severity of other non-haematological toxicities did not differ significantly between the arms. No treatment-related death was observed in this study.

Table 3 Total dose and dose intensity

	3-week regimens in this study		4-week regimen*
	IP ($n=54$) Median (range)	IPE ($n=55$) Median (range)	IPE ($n=30$) Median (range)
Total dose ($mg\,m^{-2}$)			
Cisplatin	240 (60–240)	240 (60–360)	240 (60–240)
Irinotecan	420 (60–480)	390 (60–720)	563 (60–720)
Etoposide	0	600 (150–900)	600 (150–600)
Dose intensity ($mg\,m^{-2}\,week^{-1}$)			
Cisplatin	19 (14–25)	20 (16–34)	15 (12–15)
Irinotecan	33 (14–40)	35 (15–55)	35 (19–45)
Etoposide	0	48 (34–68)	37 (28–38)

*From our previous study (Sekine *et al*, 2003).

Table 4 Grade 3–4 toxicities

	IP ($n=54$)			IPE ($n=55$)		
	Grade 3	4	3+4 (%)	Grade 3	4	3+4 (%)
Leukocytopaenia	9	1	10 (19)	18	11	29 (53)*
Neutropaenia	17	11	28 (52)	24	28	52 (95)*
Anaemia	18	0	18 (25)	16	9	25 (45)
Thrombocytopaenia	2	0	2 (4)	13	0	13 (13)†
Febrile neutropaenia	5	0	5 (9)	17	0	7 (13)
Diarrhoea	8	0	8 (15)	11	2	13 (24)
Vomiting	4	0	4 (7)	3	0	3 (5)
Fatigue	1	0	1 (2)	5	1	6 (11)‡
Hyponatraemia	9	3	12 (22)	11	2	13 (24)
AST elevation	0	0	0 (0)	3	0	3 (5)
CRN elevation	1	0	1 (2)	0	0	0 (0)

*$P<0.001$; †$P<0.01$; and ‡$P=0.054$ by χ^2 test.

Response, treatment after recurrence and survival

Four CRs and 37 partial responses (PRs) were obtained in the IP arm, resulting in the overall response rate of 76 with 95% confidence interval (CI) of 65–87%, whereas six CRs and 42 PRs were obtained in the IPE arm, and the overall response rate was 87% with a 95% CI of 79–96% ($P=0.126$). Median PFS was 4.8 months (95% CI, 4.0–5.6) in the IP and 5.4 months (95% CI, 4.8–6.0) in the IPE arm ($P=0.049$) (Figure 1A). After recurrence, 22 (44%) patients in the IP arm and 8 (16%) patients in the IPE arm received etoposide-containing chemotherapy. The MST and 1-year survival rate were 12.4 months (95% CI, 9.7–15.1) and 54.8% (95% CI, 41.4–68.2%) in the IP and 13.7 months (95% CI, 11.9–15.5) and 61.5% (95% CI, 48.6–74.4%) in the IPE arm ($P=0.52$), respectively (Figure 1B).

DISCUSSION

This study showed that the IPE regimen in a 3-week schedule with CSF support produced a promising response rate, PFS and overall survival. Haematological toxicity in the IPE arm, however, was very severe in spite of the G-CSF support with the grade 3 febrile neutropaenia noted in 31% of patients.

In comparison between the 3-week IPE regimen in this study and the 4-week IPE regimen in the previous study, the delivery of cisplatin and etoposide was improved in the 3-week IPE regimen when compared with the 4-week IPE regimen at the cost of the irinotecan total dose. The response rate and MST were 87% and 13.7 months, respectively, in the 3-week IPE regimen and 77% and 12.9 months in the previous 4-week schedule, and toxicity profiles were comparable to each other (Sekine *et al*, 2003).

The MST of 12.4 months in the IP arm in this study was comparable to that of the previous phase III study, with an MST of 12.8 months (Noda *et al*, 2002). Thus, this study showed the reproducible excellent survival outcome of patients with ED-SCLC who were treated with the IP combination. In contrast, a recent American phase III study of the PE regimen *vs* IP regimen failed to show the superiority of the IP regimen to the PE regimen; the MST

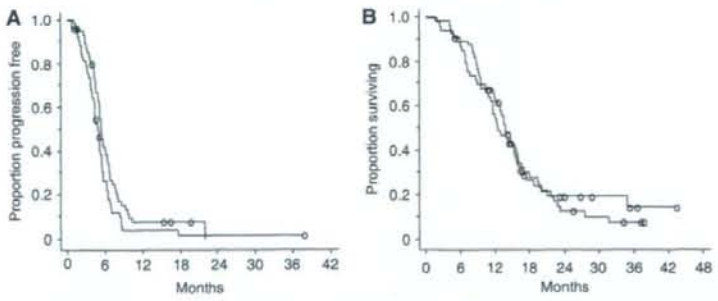

Figure 1 Progression-free survival (**A**) and overall survival (**B**). Thick line indicates the IPE regimen and thin line indicates the IP regimen.

for the PE regimen was 10.2 months and that for the IP regimen was 9.3 months (Hanna *et al*, 2006). The discrepancy between the Japanese and American trials may be explained by the different cisplatin dose schedules; cisplatin was delivered at a dose of 60 mg m^{-2} on day 1 every 3 or 4 weeks in the Japanese trials, whereas cisplatin was delivered at a dose of 30 mg m^{-2} on days 1 and 8 every 3 weeks in the American one. A platinum agent administered at divided doses was associated with poor survival in patients with ED-SCLC in our previous randomised phase II study (Sekine *et al*, 2003).

The issue of adding further agents to the standard doublet regimen has been investigated in patients with ED-SCLC. The addition of ifosfamide or cyclophosphamide and epirubicin to the cisplatin and etoposide combination produced a slight survival benefit, but at the expense of greater toxicity (Loehrer *et al*, 1995; Pujol *et al*, 2001). Phase III trials of cisplatin and etoposide with or without paclitaxel showed unacceptable toxicity with 6–13% toxic deaths in the paclitaxel-containing arm (Mavroudis *et al*, 2001; Niell *et al*, 2005). The results in these studies and the current study are consistent in the increased toxicity despite the G-CSF support and no definite survival benefit in the three or four drug combinations over the standard doublet in patients with ED-SCLC.

In conclusion, the IPE regimen was marginally more effective than the IP regimen, but was too toxic despite the administration of prophylactic G-CSF.

ACKNOWLEDGEMENTS

This study was supported, in part, by Grants-in-Aid for Cancer Research from the Ministry of Health, Labour and Welfare of Japan. We thank the following doctors for their care for patients and valuable suggestion and comments on this study: Takahiko Sugiura, Aichi Cancer Center; Yoshinobu Ohsaki, Asahikawa Medical College; Shinzo Kudoh, Osaka City University Medical School; Makoto Nishio, Cancer Institute Hospital; Hiroshi Chiba, Kumamoto Community Medical Center; Koichi Minato, Gunma Prefectural Cancer Center; Naoyuki Nogami, Shikoku Cancer Center; Hiroshi Ariyoshi, Aichi Cancer Center Aichi Hospital; Takamune Sugiura, Rinku General Medical Center; Akira Yokoyama, Niigata Cancer Center Hospital; and Koshiro Watanabe, Yokohama Municipal Citizen's Hospital. We also thank Fumiko Koh, Yuko Yabe and Mika Nagai for preparation of the paper.

REFERENCES

Armitage P, Berry G, Matthews J (2002) Survival analysis. In *Statistical Methods in Medical Research*, Armitage P, Berry G, Matthews J (eds), pp 568–590. Oxford: Blackwell Science Ltd

Fukuoka M, Furuse K, Saijo N, Nishiwaki Y, Ikegami H, Tamura T, Shimoyama M, Suemasu K (1991) Randomized trial of cyclophosphamide, doxorubicin, and vincristine *vs* cisplatin and etoposide *vs* alternation of these regimens in small-cell lung cancer. *J Natl Cancer Inst* **83:** 855–861

Hanna N, Bunn Jr PA, Langer C, Einhorn L, Guthrie Jr T, Beck T, Ansari R, Ellis P, Byrne M, Morrison M, Hariharan S, Wang B, Sandler A (2006) Randomized phase III trial comparing irinotecan/cisplatin with etoposide/cisplatin in patients with previously untreated extensive-stage disease small-cell lung cancer. *J Clin Oncol* **24:** 2038–2043

Hryniuk WM, Goodyear M (1990) The calculation of received dose intensity. *J Clin Oncol* **8:** 1935–1937

Jackman DM, Johnson BE (2005) Small-cell lung cancer. *Lancet* **366:** 1385–1396

Liu PY, Dahlberg S, Crowley J (1993) Selection designs for pilot studies based on survival. *Biometrics* **49:** 391–398

Loehrer Sr PJ, Ansari R, Gonin R, Monaco F, Fisher W, Sandler A, Einhorn LH (1995) Cisplatin plus etoposide with and without ifosfamide in extensive small-cell lung cancer: a Hoosier Oncology Group study. *J Clin Oncol* **13:** 2594–2599

Mavroudis D, Papadakis E, Veslemes M, Tsiafaki X, Stavrakakis J, Kouroussis C, Kakolyris S, Bania E, Jordanoglou J, Agelidou M, Vlachonicolis J, Georgoulias V (2001) A multicenter randomized clinical trial comparing paclitaxel–cisplatin–etoposide *vs* cisplatin–etoposide as first-line treatment in patients with small-cell lung cancer. *Ann Oncol* **12:** 463–470

Niell HB, Herndon II JE, Miller AA, Watson DM, Sandler AB, Kelly K, Marks RS, Perry MC, Ansari RH, Otterson G, Ellerton J, Vokes EE, Green MR (2005) Randomized phase III intergroup trial of etoposide and cisplatin with or without paclitaxel and granulocyte colony-stimulating factor in patients with extensive-stage small-cell lung cancer: Cancer and Leukemia Group B Trial 9732. *J Clin Oncol* **23:** 3752–3759

Noda K, Nishiwaki Y, Kawahara M, Negoro S, Sugiura T, Yokoyama A, Fukuoka M, Mori K, Watanabe K, Tamura T, Yamamoto S, Saijo N (2002) Irinotecan plus cisplatin compared with etoposide plus cisplatin for extensive small-cell lung cancer. *N Engl J Med* **346:** 85–91

Pujol JL, Daures JP, Riviere A, Quoix E, Westeel V, Quantin X, Breton JL, Lemarie E, Poudenx M, Milleron B, Moro D, Debieuvre D, Le Chevalier T (2001) Etoposide plus cisplatin with or without the combination of 4′-epidoxorubicin plus cyclophosphamide in treatment of extensive small-cell lung cancer: a French Federation of Cancer Institutes multicenter phase III randomized study. *J Natl Cancer Inst* **93:** 300–308

Roth BJ, Johnson DH, Einhorn LH, Schacter LP, Cherng NC, Cohen HJ, Crawford J, Randolph JA, Goodlow JL, Broun GO, Omura GA, Greco FA (1992) Randomized study of cyclophosphamide, doxorubicin, and vincristine *vs* etoposide and cisplatin *vs* alternation of these two regimens in extensive small-cell lung cancer: a phase III trial of the Southeastern Cancer Study Group. *J Clin Oncol* **10:** 282–291

Sekine I, Nishiwaki Y, Noda K, Kudoh S, Fukuoka M, Mori K, Negoro S, Yokoyama A, Matsui K, Ohsaki Y, Nakano T, Saijo N (2003) Randomized phase II study of cisplatin, irinotecan and etoposide combinations administered weekly or every 4 weeks for extensive small-cell lung cancer (JCOG9902-DI). *Ann Oncol* **14:** 709–714

Therasse P, Arbuck SG, Eisenhauer EA, Wanders J, Kaplan RS, Rubinstein L, Verweij J, Van Glabbeke M, van Oosterom AT, Christian MC, Gwyther SG (2000) New guidelines to evaluate the response to treatment in solid tumors. European Organization for Research and Treatment of Cancer, National Cancer Institute of the United States, National Cancer Institute of Canada. *J Natl Cancer Inst* **92:** 205–216

Lung Cancer (2008) 62, 45–54

available at www.sciencedirect.com

ScienceDirect

journal homepage: www.elsevier.com/locate/lungcan

Megakaryocyte potentiating factor as a tumor marker of malignant pleural mesothelioma: Evaluation in comparison with mesothelin

Kota Iwahori[a,b], Tadashi Osaki[a,*], Satoshi Serada[b], Minoru Fujimoto[b], Hidekazu Suzuki[c], Yoshiro Kishi[d], Akihito Yokoyama[e], Hironobu Hamada[f], Yoshihiro Fujii[d], Kentaro Yamaguchi[g], Tomonori Hirashima[c], Kaoru Matsui[c], Isao Tachibana[a], Yusuke Nakamura[h], Ichiro Kawase[a], Tetsuji Naka[b]

[a] *Department of Respiratory Medicine, Allergy, and Rheumatic Diseases, Osaka University Graduate School of Medicine, 2-2 Yamada-oka, Suita, Osaka 565-0871, Japan*
[b] *Laboratory for Immune Signal, National Institute of Biomedical Innovation, 7-6-8 Saito-Asagi, Ibaraki, Osaka 567-0085, Japan*
[c] *Department of Thoracic Malignancy, Osaka Prefectural Medical Center for Respiratory and Allergic Diseases, 3-7-1 Habikino, Habikino, Osaka 583-8588, Japan*
[d] *Department of Research and Development, Ina Institute, Medical & Biological Laboratories, Co., Ltd., 1063-103 Terasawaoka, Ina, Nagano 396-0002, Japan*
[e] *Department of Hematology and Respiratory Medicine, Kochi University, 185-1, Okohchou-kohatu, Nanngoku, Kohchi 783-8505, Japan*
[f] *Department of Integrated Medicine and Informatics, Ehime University Graduate School of Medicine, Sizukawa, Ohonn, Ehime 791-0295, Japan*
[g] *Department of Product Development, Ina Institute, Medical & Biological Laboratories, Co., Ltd., 1063-103 Terasawaoka, Ina, Nagano 396-0002, Japan*
[h] *Laboratory of Molecular Medicine, Human Genome Center, Institute of Medical Science, The University of Tokyo, 4-6-1 Shirokanedai, Minato-ku, Tokyo 108-8639, Japan*

Received 30 October 2007; received in revised form 30 January 2008; accepted 14 February 2008

KEYWORDS
Mesothelioma;
Megakaryocyte potentiating factor;
Mesothelin;
Tumor markers

Summary
Purpose: An early and reliable blood test is one deficiency in diagnosis of malignant pleural mesothelioma (MPM). Megakaryocyte potentiating factor (MPF) and mesothelin variants (MSLN), members of the mesothelin gene family, have been studied as candidate serum markers for MPM. We developed a novel enzyme-linked immunosorbent assay (ELISA) system to compare the diagnostic efficacy of MPF and MSLN in MPM and control groups.
Experimental design: MPF and MSLN were assayed with ELISA in 27 consecutive MPM patients and 129 controls including patients with lung cancer and asymptomatic asbestos-exposed subjects.

Abbreviations: MPM, malignant pleural mesothelioma; MPF, megakaryocyte potentiating factor; MSLN, mesothelin variants 1 and 3; ELISA, enzyme-linked immunosorbent assay.

* Corresponding author. Tel.: +81 6 6879 3833; fax: +81 6 6879 3839.
E-mail address: osaki@imed3.med.osaka-u.ac.jp (T. Osaki).

0169-5002/$ – see front matter
doi:10.1016/j.lungcan.2008.02.012

Results: Statistically significant elevation of serum MPF and MSLN levels was noted in MPM patients in comparison with every control group. The area under the receiver operating characteristic curve (AUC) was calculated for differentiation of MPM and lung cancer, healthy asbestos-exposed subjects, and healthy adults. While the AUC for serum MPF was 0.879, cut-off = 19.1 ng/ml (sensitivity = 74.1%, specificity = 90.4%), the AUC for serum MSLN was 0.713, cut-off = 93.5 ng/ml (sensitivity = 59.3%, specificity = 86.2%). Comparison between AUC for MPF and MSLN values shows that MPF is significantly superior to MSLN ($p = 0.025$). Finally, there was a significant correlation between MPF and MSLN values for MPM (Pearson's correlation coefficient = 0.77; $p < 0.001$).

Conclusions: These findings suggest that diagnostic value of MPF for MPM was better than that of MSLN although both markers showed almost equal specificity for MPM.

1. Introduction

Malignant pleural mesothelioma (MPM) is an aggressive tumor arising from mesothelial cells of serosal cavities. MPM may be asymptomatic at an early stage and is sometimes discovered by routine chest radiography. Common symptoms include chest pain and dyspnea, which are caused by tumor invasion of the chest wall or pleural effusion, and occur late during the disease progression. Although pemetrexed improves survival of unresectable MPM patients, overall median survival is only 12.1 months [1]. MPM is thought to be curable by early radical resection in combination with adjuvant chemoradiotherapy [2]. Even if surgical resection is not applicable, the early use of chemotherapy offers a prolonged period of symptom control and survival. MPM is often associated with past exposure to asbestos. There is a long latency period, often exceeding 20 years, between first exposure to asbestos and diagnosis of MPM [3]. The number of deaths from MPM is expected to increase in the next 20 years in Europe, Japan and Australia, where heavy use of asbestos has occurred [3–6]. There is thus a growing need for sensitive markers that can detect MPM in people at risk for this disease.

A 40-kDa membrane-bound mesothelin and a 31-kDa soluble megakaryocyte potentiating factor (MPF) originate from the same 69-kDa glycosyl-phosphatidylinositol-linked (GPI) glycoprotein precursor [7]. Mesothelin comprises three soluble forms of variants (MSLN). Variant 1 is a predominant mRNA expressed by both normal and tumor cells and its product is detectable in the ascites from ovarian cancer patients. It is thought to be proteolytically cleaved from the cell surface. Soluble variant 3 was detected as a small percentage of total mesothelin products from cell lines and tissues [8,9].

Scholler et al. prepared a monoclonal antibody, OV569, by immunizing mice with ovarian carcinoma cells. OV569 identified a 42- to 45-kDa protein with an N-terminal amino acid sequence identical to that of the membrane-bound portion of mesothelin and MPF, which was designated as soluble mesothelin related proteins (SMRP) [10]. A study utilizing OV569 showed an increase in SMRP concentrations in 37 of 44 patients (84%) with MPM [11]. The commercial assay kit for SMRP is designed to recognize the sequence within membrane-bound mesothelin and thus to measure mesothelin variants 1 and 3 [9]. SMRP is, therefore, identical to MSLN [11].

Later, Shiomi et al. showed that MPF is also secreted into the blood of mesothelioma patients and that the median levels of MPF in those patients were substantially elevated than in those in controls [12]. Onda et al. reported that serum MPF was elevated in 91% (51 of 56) of patients with mesothelioma and that measuring MPF may be useful for monitoring the response of mesothelioma to treatment [13]. Mesothelin variants and MPF thus appear to be promising targets for MPM diagnosis.

However, it has not yet been established whether MPF or MSLN is a more effective marker for differential diagnosis of MPM. To this end, we generated monoclonal antibodies (mAb) and prepared two enzyme-linked immunosorbent assay (ELISA) systems that each recognizes MPF or MSLN. In this paper we report the results of our studies comparing the discriminatory potency of MPF with that of MSLN for diagnosis of MPM.

2. Materials and methods

2.1. Patients and controls

Serum samples were collected from 27 consecutive patients with non-resectable MPM, whose diagnosis was confirmed by cytological or histopathological examination by pathologists skilled in diagnosis of this disease. The patient population included 13 with epithelial type MPM, three with sarcomatoid type, 5 with mixed type and 6 with unclassified type (diagnosed by cytological analysis). For control, we used 47 patients with lung cancer, 35 with other cancers (18 ovarian, 8 stomach and 9 colon cancers), 9 asbestos-exposed asymptomatic subjects and 38 healthy adults without a history of asbestos exposure. We obtained written and oral informed consent from all participants. This study was approved by our institutional review board.

2.2. Antigen preparation

Recombinant MPF protein was produced by amplifying the part coding for amino acids 1–288 from the cDNA encoding the transcript variant 1 for human mesothelin (Genbank accession no. NM_005823) with DNA polymerase

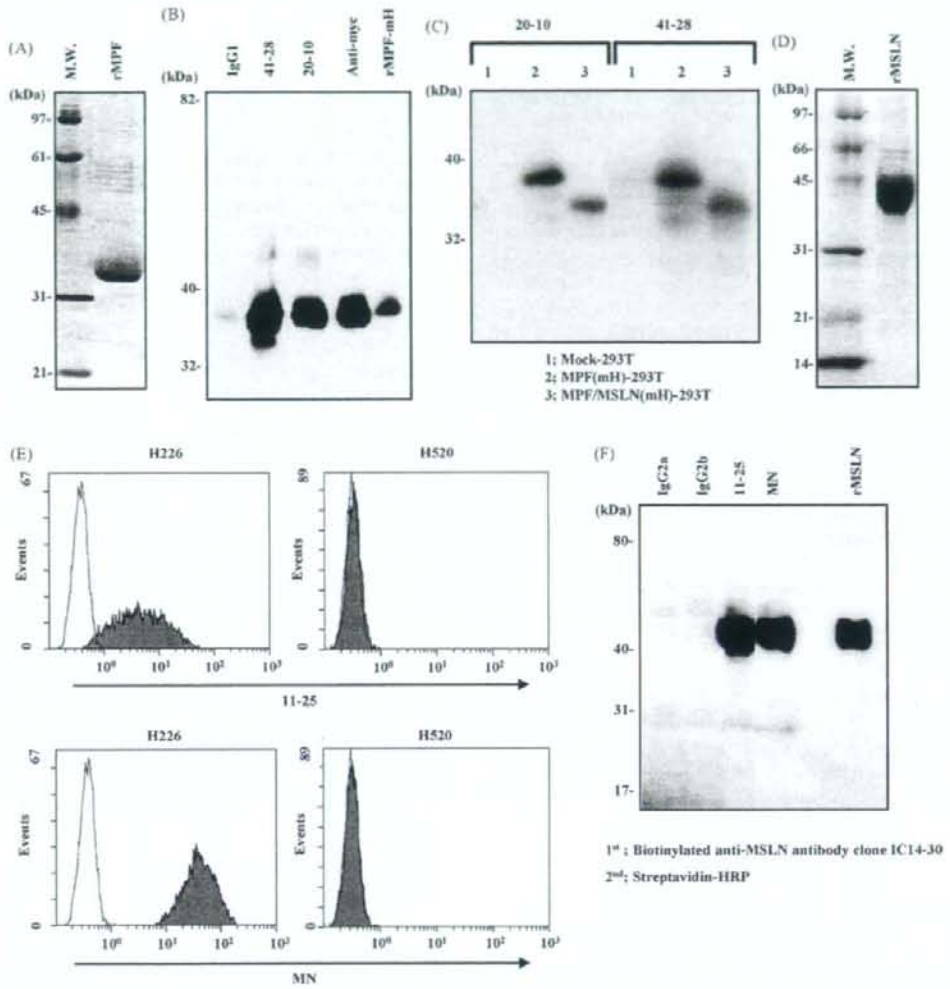

Fig. 1 Characterization of anti-Megakaryocyte potentiating factor (MPF) and anti-mesothelin variants (MSLN) antibodies. (A and D) Purity of the prepared recombinant MPF (A) and MSLN (D) proteins for immunization. Proteins were electrophoresed under reduced condition and stained with Coomassie Brilliant Blue. (B and F) Reactivity of anti-MPF antibodies to recombinant MPF protein (B) or anti-MSLN antibodies to MSLN in the culture supernatant of NCI-H226 cells (F). Anti-MPF antibodies (B, lanes 41–28 and 20–10) or anti-MSLN antibodies (F, lanes 11–25 and MN) were used for immunoprecipitation. Recovered proteins were separated by SDS-PAGE and electrotransfered to polyvinylidenefluoride (PVDF) membranes. Membranes were probed with anti-myc antibody for myc-His tagged MPF or anti-MSLN antibody clone IC14–30 for MSLN, respectively, and followed by development. Recombinant MPF protein (B, lane rMPF-mH) or recombinant MSLN protein (F, lane rMSLN) were applied for positive controls. (C), western blot analysis of anti-MPF antibodies. Supernatants of the HEK 293T transfectants with myc-His tagged MPF, full length of mesothelin variant 1 or mock vectors were separated by SDS-PAGE and electrotransfered to a PVDF membrane. The membrane was probed with anti-MPF antibodies (20–10 and 41–28), incubated with HRP-labeled anti-mouse IgG antibody and followed by chemiluminescence. Lane 1, Mock-transfected 293T; lane 2, myc-His tagged MPF-transfected 293T; lane 3, full length of mesothelin variant 1-transfected 293T. (E), expression of mesothelin on the surface of lung cancer cell lines. NCI-H226 and NCI-H520 were incubated with anti-MSLN antibodies (11–25 and MN) or an isotype-matched control antibody and followed by PE-conjugate anti mouse IgG. Antigen expression was detected by flow cytometry.

(recombinant Taq polymerase; Takara Bio Inc., Shiga, Japan) and using the primers 5′-CGGAATTCGCCGCCACC-ATGGCCTTGCCAACGGCTCGACCCCTGTTG-3′ and 5′-GCTCT-AGAGATGGTCCGTTCAGGCTGCCGCCAGGATGG-3′. The amplified DNA was inserted into the EcoRI/XbaI site of mammalian expression plasmid pcDNA3.1/myc-His (Invitrogen, Carlsbad, CA) and transfected into HEK 293T cells by lipofection (Lipofectamine2000; Invitrogen). The culture supernatant was applied to a TALON resin according to the manufacturer's instructions (Clontech, Mountain View, CA). The purified MPF protein thus obtained was dialyzed with 4.0 liter of PBS twice and kept frozen at −80 °C until use as an immunogen or as a standard polypeptide for sandwich ELISA. Purity of the recombinant MPF was confirmed by Coomassie Brilliant Blue staining after electrophoresis under reduced condition (Fig. 1A).

MSLN was produced by amplifying the part coding for amino acids 297–580 of the same cDNA and using the primers 5′-AAATTTCCCAAGCTTGTGGAGAAGACAGCCTGTCCTTCAG-GCAAG-3′ and 5′-AAGGAAAAAAGCGGCCGCGCCCTGTAGCC-CCAGCCCCAGCGTGTCCAG-3′. The amplified DNA was inserted into the HindIII/NotI site of expression vector pSecTag2B (Invitrogen). It should be noted that variants 1 and 3 of mesothelin share amino acids 297–580 of clone NM_005823 as a common sequence. The plasmid DNA was transfected into HEK 293T cells, and recombinant MSLN produced in the culture supernatant was purified and stored as above (Fig. 1D).

2.3. Antibody generation

To generate mAbs against MPF and against MSLN, 4- to 6-week old BALB/c mice were immunized with the respective purified protein i.p. on days 0, 7, 14, and 16 (10 μg/shot). Following the last immunization, lymphocytes of the spleen were collected and fused with P3U1 myeloma cells in a 50% polyethylene glycol 4000 solution (Wako, Osaka, Japan) on day 18. The fused cells were plated on 96-well plates with RPMI-1640 medium containing 15% fetal calf serum (FCS; Equitech-Bio Inc., Kerrville, TX), penicillin/streptomycin (Invitrogen) and HAT solution (Invitrogen). After 10 days incubation at 37 °C with 5% CO_2 in a humidified environment, culture supernatants were collected and screened for their ability to bind to the immunizing antigen by means of an indirect ELISA using recombinant MPF or soluble mesothelin, respectively. Selected positive hybridoma colonies were expanded and subcloned by limiting dilution. An isostrip kit (Hoffmann-La Roche, Basel, Switzerland) was used for antibody isotype determination according to the manufacturer's instructions. Antibody purification was carried out with protein A affinity chromatography (GE Healthcare, Buckinghamshire, UK). Following a competition assay for the immunogens among the clones thus obtained (data not shown), clone 20–10 (IgG1 κ) and clone 41–28 (IgG1 κ) were selected to construct an sandwich ELISA for the detection of MPF, while MN (IgG2a κ) and 11–25 (IgG2b κ) were chosen for construction of an MSLN ELISA as described elsewhere. Clone MN was previously obtained by Dr. Ira Pastan's laboratory as a specific monoclonal antibody against mesothelin [14] and used in this study under a licensing agreement with NIH. Clones 41–28 and 11–25 were biotinylated using ECL Protein Biotination Module (GE Healthcare).

2.4. Flow cytometry

Lung cancer cell lines NCI-H226 and NCI-H520 were cultured in RPMI medium (SIGMA) supplemented with 10% fetal bovine serum. The former cell line expresses both MPF and MSLN but the latter does neither [14]. After a treatment with PBS containing 5 mM EDTA for 3 min, detached cells were washed with PBS twice and incubated with 1 μg/ml of anti-MSLN Abs or isotype-matched controls for 30 min at 4 °C in PBS containing 0.5% BSA and 2mM EDTA. Following twice wash with the above buffer, PE-conjugate anti-mouse IgG was added and further incubated for 30 min at 4 °C. All flow cytometry was performed on Cytomics FC500 (Beckman Coulter).

2.5. Immunoprecipitation

The reactivity of anti-MPF Abs to recombinant MPF protein, or anti-MSLN Abs to recombinant MSLN protein in the culture supernatant of NCI-H226 was confirmed by immunoprecipitation. 15 μl of Protein G sepharose suspended in PBS containing 0.01% BSA (SIGMA) was incubated with 5 μg of anti-MPF Abs 20–10 and 41–28, or anti-MSLN Abs 11–25 and MN, for 2 h at 4 °C with gently rocking. During this step, 250 ng of the recombinant myc-His tagged MPF protein or 5 times concentrated culture supernatant of NCI-H226 and NCI-H520 were incubated with Protein G beads for 30 min at 4 °C with shaking to preclear the samples. The Protein G sepharose incubated with the antibodies were centrifuged at 1000 × *g* for 2 min and washed with PBS 3 times. Then the precleared samples were added to the tube containing the washed Protein G sepharose and rotated for over night at 4 °C. After the incubation, the beads were washed with PBS 3 times and boiled in 25 μl of 2× Laemmli's SDS sample buffer for 5 min. Proteins (20 μl of sample per lane) were separated by sodium dodecylsulfate-polyacrylamide gel electrophoresis (SDS-PAGE) on a 12.5% polyacrylamide gel and electrotransfered to a polyvinylidenefluoride (PVDF) membrane. The membrane blocked with 5% nonfat milk in PBS containing 0.05% Tween-20 (blocking buffer) was incubated with 1.0 μg/ml mouse anti-myc mAb (MBL) for detecting myc-His tagged MPF, or 1.0 μg/ml biotinylated anti-MSLN antibody clone IC14–30 (MBL) for detecting MSLN for 1 h at room temperature. After 4 times wash with PBS containing 0.05% Tween-20, the membrane was incubated with a horseradish peroxidase (HRP)-conjugated anti-mouse IgG (MBL) for MPF diluted 1:5000 with the blocking buffer or HRP-streptavidin (GE Amersham) for MSLN diluted 1:5000 with the blocking buffer. The chemiluminescence was developed by according to manufacture's procedure (ECL; GE Amersham). 50 ng of recombinant MPF protein or 250 ng of recombinant MSLN protein was applied as a positive control for Western blotting.

2.6. Western blot

HEK 293T cells were transfected by lipofection with expression vectors coding myc-His tagged MPF, full length of

mesothelin variant 1, or a mock vector as a negative control, and the culture media were collected after 72 h-incubation in a CO_2 incubator at 37 °C. Supernatants of the media were recovered by a centrifugation at 3000 × *g* for 10 min at room temperature, and then boiled with an equal volume of 2× SDS sample buffer for 5 min. 20 μl of samples per lane were loaded on a 12.5% SDS-polyacrylamide gel and separated by SDS-PAGE. After electrotransfer to a PVDF membrane, the membrane was treated with the blocking buffer containing 5% nonfat milk and incubated with 2.0 μg/ml anti-MPF Abs (20–10 and 41–28) for 1 h at room temperature. After 4 times wash with PBS containing 0.05% Tween-20, the membrane was incubated with HRP-labeled anti-mouse IgG (MBL) diluted 1:5000 with the blocking buffer. The chemiluminescence was done by according to manufacture's procedure (ECL; GE Amersham).

2.7. Sandwich ELISA

The serum concentrations of MPF and of the soluble form of mesothelin were measured by each specific sandwich ELISA constructed as follows: 96-well microtiter plates (Maxisorp; Nalgen Nunc International Corp., Rochester, NY) were coated with the capturing antibody, clone 20–10 for MPF or clone MN for MSLN, and adjusted to 5 μg/ml with 100 mM carbonate buffer (pH 9.6) at 4 °C overnight. The plates were blocked with 200 μl PBS (pH 7.4) containing 1.0% BSA, 5.0% sucrose, and 0.1% NaN_3 for 2 h and then incubated for 1 h with serum samples diluted to 1:40 with PBS (pH 7.4) containing 1.0% BSA, 0.1% Tween20, 50 μg/ml MAK33 (Roche), and 0.1% NaN_3. After washing with PBS (pH 6.7) containing 0.13% Tween-20, the wells were incubated for 1 h with 2.0 μg/ml biotinylated mAb 41–28 for detecting MPF, or incubated with 0.7 μg/ml biotinylated mAb 11–25 for detecting soluble mesothelin, and reacted with streptavidin-conjugated peroxidase (GE Healthcare) diluted to 1:60,000 for MPF or avidin-conjugated peroxidase (DAKO, Glostrup, Denmark) diluted to 1:10,000 for soluble mesothelin, respectively, with 20 mM HEPES (pH 6.5) containing 1.0% BSA, 0.135 M NaCl, 0.1% *p*-hydroxy phenyl acetic acid (Tokyo Chemical Industry, Tokyo, Japan), and 0.15% ProClin150 (Supelco, St. Louis, MO). Followed by four washes with PBS, 50 μl/well TMB (Moss Inc., Pasadena, MD) was added and the plates were incubated for 30 min. The color development was stopped by the addition of 0.36N H_2SO_4. Color intensity was determined with a microplate reader Model 680 (Bio-Rad Laboratories, Hercules, CA) at a wavelength of 450 nm with a reference wavelength of 620 nm. Analyte concentrations were calculated by referring to the standard curve using serial diluted recombinant MPF or MSLN, respectively (Fig. 2A for MPF and Fig. 2B for MSLN).

2.8. Statistical analyses

Nonparametric Mann Whitney's U test was used for comparison of the data. $p < 0.05$ was considered statistically significant. For drawing of receiver operating characteristic (ROC) curves and estimation of the area under the ROC curve (AUC) statistics software SPBS (Comworks, Saitama, Japan) was used to quantify the ability to differentiate between healthy volunteers and patients with indicated diseases. Pearson's correlation coefficient was calculated to determine the correlation between MPF and MSLN.

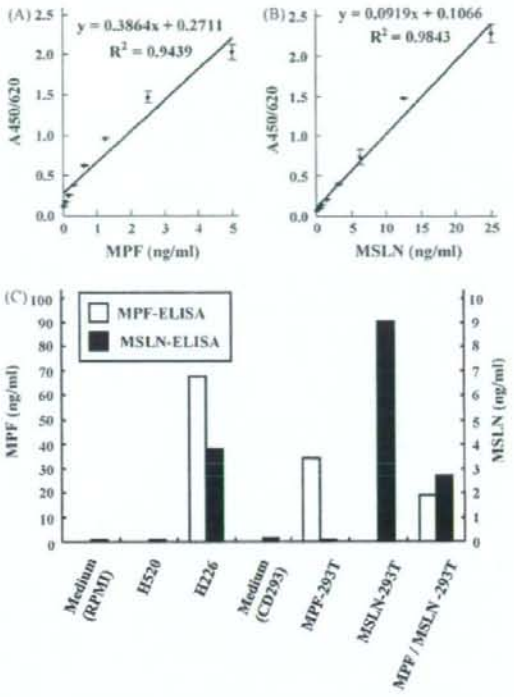

Fig. 2 Sandwich ELISA. Standard curves for MPF (A) and MSLN (B). ELISAs displaying the mean absorbance values from indicated concentrations of recombinant proteins. Points, mean; bars, S.D. (C), MPF and MSLN levels in the supernatants of cell lines and 293 transfectants measured by specific ELISA systems. The levels in the supernatants of 293 transfectants are indicated as those of 500 times diluted solution. Open bars, MPF; closed bars, MSLN.

3. Results

3.1. Generation of sandwich ELISA specific for MPF and soluble mesothelin (MSLN)

To generate mAbs that specifically react with MPF, recombinant MPF protein corresponding to the amino acids 1–288 from the transcript variant 1 of human mesothelin was produced by 293T transfectants (Fig. 1A) and immunized to BALB/c mice. Supernatants of obtained hybridomas were tested for the binding activity to the microplate coated with immunizing antigen and further examined by a competition assay for the immunogen (data not shown). The specific reactivities of selected clone 20–10 and clone 41–28 to MPF were checked by immunoprecipitation using myc-His tagged recombinant MPF (Fig. 1B), and also performed by Western blot using the supernatants of 293T cells transfected with

expression vectors coding myc-His tagged MPF (Fig. 1C, lane 2) and the full length of mesothelin variant 1 (Fig. 1C, lane 3). A smaller band on lane 3 compared to the myc-His tagged MPF on lane 2 were detected by both anti-MPF Abs. MPF and mesothelin are produced together as a precursor form. Following cleavage by a protease furin, MPF is released as an N-terminal 31-kDa fragment from mesothelin [15]. The smaller band on the lane 3 seems to be the 31-kDa mature form of MPF without myc-His Tag. A sandwich ELISA for MPF was constructed using the anti-MPF antibodies 20–10 and 41–28. The standard curve using purified recombinant MPF was shown in Fig. 2A. Correlated with Fig. 1C, the MPF sandwich ELISA detected the antigen in the culture supernatant of the 293T transfectant expressing the full length of mesothelin variant 1 (Fig. 2C, MPF/MSLN-293T), as well as MPF-transfected cells (Fig. 2C, MPF-293T) but not the soluble mesothelin secreted in the culture supernatant of the MSLN-transfectants (Fig. 2C, MSLN-293T).

The monoclonal anti-MSLN antibody, clone 11–25, were generated by immunizing mice with recombinant MSLN (amino acids 297–580 of mesothelin variant 1). The specificity of 11–25 to MSLN was tested using a lung cancer cell line, NCI-H226, which has been clarified to express mesothelin [14]. 11–25 detected not only the antigen on the cell surface of NCI-H226 by flowcytometory (Fig. 1E, upper left panel), but also identified soluble antigen in the culture supernatant of NCI-H226 by immunoprecipitation (Fig. 1F, lane 11–25). Another anti-MSLN Ab, clone MN, which the Pastan's laboratory has previously developed, was used, in combination with 11–25, to establish a sandwich ELISA for MSLN [14]. The standard curve using recombinant MSLN was shown in Fig. 2B. The MSLN sandwich ELISA recognized the soluble antigen in the culture supernatant of NCI-H226 (Fig. 2C, H226) as well as the 293T transfectant expressing the full length of mesothelin variant1 (Fig. 2C, MPF/MSLN-293T). On the other hands, this MSLN ELISA did not detect recombinant MPF in the culture supernatant of the MPF-transfectants (Fig. 2C, MPF-293T).

3.2. MPF and MSLN in blood samples

We measured serum MPF and MSLN levels in all subjects. Serum MPF levels differed among the five groups (Fig. 3A and Table 1), with mean serum MPF values were higher for MPM patients (68.7 ± 101.1 ng/ml [mean ± standard deviation]) than for patients with lung cancer (16.6 ± 15.3 ng/ml), individuals with other cancers (15.1 ± 9.7 ng/ml), healthy asbestos-exposed subjects (9.7 ± 5.3 ng/ml) and healthy adults (9.0 ± 2.9 ng/ml). The difference in median values between MPM and every control group was statistically significant (Mann–Whitney's U test; $p < 0.001$). Mean serum MSLN levels in MPM, patients with lung cancer, individuals with other cancers, healthy asbestos-exposed subjects, or healthy adults were 130.0 ± 112.9 ng/ml, 83.4 ± 50.4 ng/ml, 74.4 ± 45.3 ng/ml, 59.5 ± 25.6 ng/ml and 61.4 ± 21.4 ng/ml, respectively (Fig. 3B and Table 1). The median serum MSLN level of MPM was significantly higher than in the control groups (Mann–Whitney's U test; MPM *vs.* lung cancer: $p = 0.028$, MPM *vs.* other cancers: $p = 0.005$, MPM *vs.* asbestos-exposed subjects: $p = 0.010$, MPM *vs.* healthy adults: $p < 0.001$). There was no significant difference in MPF or MSLN levels among MPM patients with different histologies (Table 1).

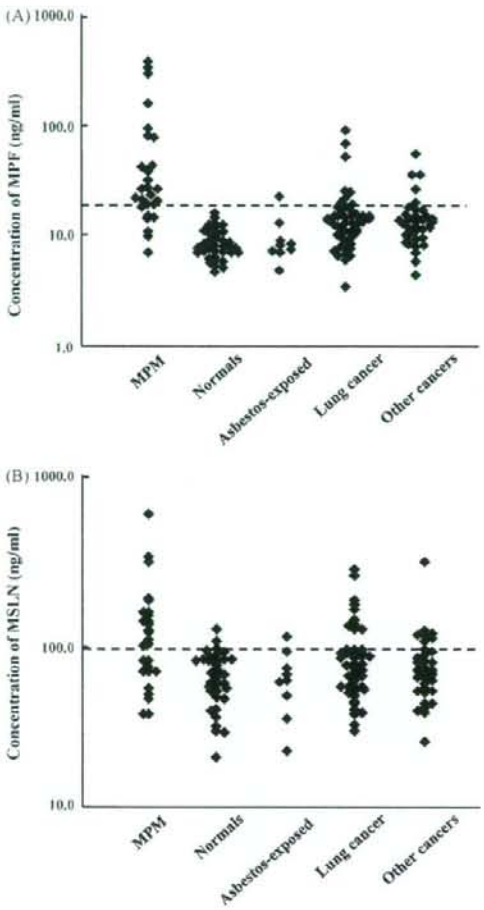

Fig. 3 Megakaryocyte potentiating factor (MPF) (A) and mesothelin variants (MSLN) (B) levels in the sera of malignant pleural mesothelioma (MPM) patients and control groups. Each dot represents one patient. The horizontal broken lines represent cut-off values: 19.1 ng/ml for MPF and 93.5 ng/ml for MSLN. MPM, malignant pleural mesothelioma; Normals, healthy volunteers; Asbestos-exposed, asbestos-exposed asymptomatic individuals; other cancers, ovarian, stomach and colon cancer patients.

3.3. Cut-off value, sensitivities and specificities calculation of MPF and MSLN

To assess the clinical potential of MPF, we compared sensitivities and specificities of MPF with those of MSLN. The operating characteristics for the two tumor markers with their cut-off points for achieving the best individual accuracy are shown in Fig. 4A. The area under the receiver operating characteristic (ROC) curve (AUC) for serum MPF

Table 1 Serum concentrations of megakaryocyte potentiating factor (MPF) and mesothelin variants (MSLN) in mesothelioma patients and controls

Diagnosis	Number of study participants	MPF (ng/ml)			MSLN (ng/ml)		
		Mean (S.D.)	Median	Range	Mean (S.D.)	Median	Range
MPM	27	68.7 (101.1)	26.3	6.9–370.1	130.0 (112.9)	101.5	35.9–576.1
Epithelial type	13	87.4 (112.6)	38.1	14.2–370.1	132.2 (67.7)	129.3	64.8–317.8
Sarcomatoid type	3	16.5 (5.8)	19.1	9.8–20.4	67.9 (38.6)	57.3	44.5–112.4
Mixed type	5	77.7 (143.7)	14.8	6.9–334.6	158.8 (233.6)	65.2	35.9–576.1
Unclassified type	6	47.0 (54.3)	24.7	15.3–156.3	132.3 (88.9)	109.7	35.9–296.6
Malignant condition							
Lung cancer	47	16.6 (15.3)	13.3*	3.4–89.4	83.4 (50.4)	70.7†	28.6–267.8
Other cancers	35	15.1 (9.7)	13.0‡	4.4–54.5	74.4 (45.3)	66.4‖	24.6–298.2
Ovarian cancer	18	18.0 (12.5)	13.7	4.4–54.5	83.2 (56.9)	67.8	41.7–298.2
Stomach cancer	8	14.3 (3.7)	14.1	9.6–19.7	73.9 (29.0)	69.9	36.9–113.8
Colon cancer	9	9.7 (2.9)	8.7	5.8–14.0	57.0 (24.5)	51.6	24.6–106.6
Asbestos-exposed individuals	9	9.7 (5.3)	8.2¶	4.9–22.7	59.5 (25.6)	56.7§	21.6–106.0
Healthy volunteers	38	9.0 (2.9)	8.0#	4.8–16.6	61.4 (21.4)	62.0#	19.6–117.4

* Significance of median values for the specified control groups compared with MPM. Mann–Whitney's *U* test; $p < 0.001$.
† Significance of median values for the specified control groups compared with MPM. Mann–Whitney's *U* test; $p = 0.028$.
‡ Significance of median values for the specified control groups compared with MPM. Mann–Whitney's *U* test; $p = 0.005$.
§ Significance of median values for the specified control groups compared with MPM. Mann–Whitney's *U* test; $p = 0.01$.

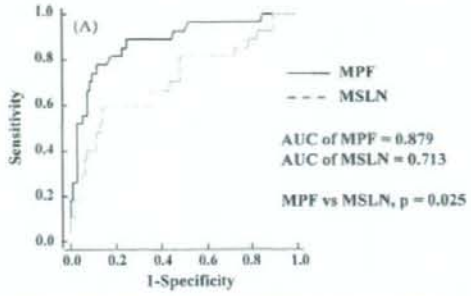

Marker	Cut-off (ng/ml) (n=94)	Sensitivity (%)	Specificity (%)
MPF	19.1	74.1	90.4
MSLN	93.5	59.3	86.2

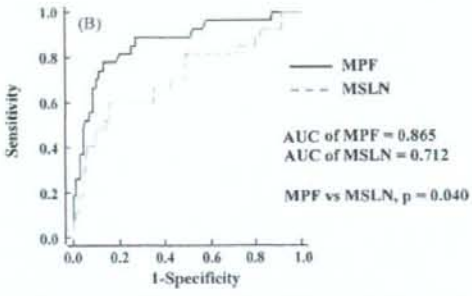

Marker	Cut-off (ng/ml) (n=129)	Sensitivity (%)	Specificity (%)
MPF	19.1	74.1	89.1
MSLN	123.7	40.7	93.8

Fig. 4 Receiver operating characteristic (ROC) curves for megakaryocyte potentiating factor (MPF) and mesothelin variants (MSLN) for differentiation between malignant pleural mesothelioma ($n = 27$) and controls. Controls comprise lung cancer patients ($n = 47$), asbestos-exposed asymptomatic individuals ($n = 9$) and healthy volunteers ($n = 38$) for (A). For the analysis shown in (B), control groups include other cancers ($n = 35$) in addition to those specified in (A). The tables show the best statistical cut-off values for MPF and MSLN with pairs of sensitivity and specificity.

was 0.879 for differentiating MPM patients from controls comprising lung cancer patients, asbestos-exposed individuals and healthy adults, with a cut-off value of 19.1 ng/ml (sensitivity = 74.1%, specificity = 90.4%), whereas the AUC for serum MSLN was 0.713 with a cut-off value of 93.5 ng/ml (sensitivity = 59.3%, specificity = 86.2%) (Fig. 4A). Serum MPF levels were elevated in 20 (74.1%) MPM patients, eight (17.0%) lung cancer patients and five (14.3%) individuals with other cancers (Fig. 3A). Corresponding serum MSLN levels were elevated in 59.3%, 21.3% and 20.0% of the patients (Fig. 3B). Both MPF and MSLN showed elevated levels in

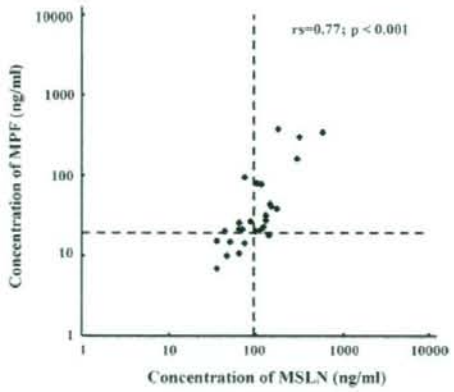

Fig. 5 Inter-marker correlation between megakaryocyte potentiating factor (MPF) and mesothelin variants (MSLN) for malignant pleural mesothelioma (MPM). Each dot indicates MPF and MSLN values for the same MPM patient ($n = 27$). r_s, Pearson's correlation coefficient. The horizontal dotted line represents the cut-off value for MPM (19.1 ng/ml) and the vertical dotted line for MSLN (93.5 ng/ml).

four (22.2%) ovarian cancer patients, while MPF values were elevated in one (11.1%) asbestos-exposed adult and none of the healthy donors, and MSLN levels were elevated in one (11.1%) asbestos-exposed adult and two (5.3%) healthy donors. Calculation of areas under the ROC curves showed a significant difference between the two markers ($p = 0.025$) (Fig. 4A). ROC curves for a comparison of MPM with all non-MPM patients and healthy adults, yielded an AUC of 0.865 for MPF and of 0.712 for MSLN (MPF *vs.* mesothelin, $p = 0.04$) (Fig. 4B). Sensitivity of MSLN decreased to 40.7% while that of MPF did not change (Fig. 4B). Comparison of the AUC values thus showed a better diagnostic performance by MPF than MSLN for discriminating MPM.

3.4. Inter-marker correlation

To examine inter-marker correlation between MPF and MSLN values for MPM, we plotted concentrations of MPF and MSLN in the same figure (Fig. 5) and found a significant correlation between MPF and MSLN values for MPM (Pearson's correlation coefficient, $r_s = 0.77$; $p < 0.001$). Concentrations for six patients were above the cut-off value for MPF (19.1 ng/ml) but below the cut-off values (93.5 ng/ml) for MSLN, whereas only one showed the opposite condition. Concentrations for 14 patients were above the cut-off values for both markers and for six patients they were below these values (Fig. 5).

4. Discussion

Recent studies identified increased levels of MSLN in the blood of MPM [11,16–18] and other histological cancer patients [9,10]. They suggested MSLN was useful for diagnosis of MPM and for monitoring disease progression. Recently, MPM patients were found to have raised serum concentrations of MPF [13,19], indicating that MPF can also be a candidate diagnostic marker for MPM. To determine which molecule, MPF or MSLN, is more sensitive for screening of MPM, we developed two novel sets of ELISA system. The one for MSLN recognizes mesothelin variants 1 and 3. In our study, higher MPF levels were found in 74.1% of MPM patients and elevated MSLN levels in 59.3%. Scherpereel et al. demonstrated that MPM epithelioid type had significant elevated values for MSLN than mixed type or sarcomatoid type [17]. Nevertheless, we and Creaney et al. did not find significant difference in levels of either MSLN or MPF in MPM patients with different histologies (Table 1) [20]. The sensitivity of 59.3% of MSLN established in our study was comparable to the sensitivity of 52% in Creaney' s study of 117 MPM patients [20] or 68% of Cristaudo' s study [21]. Regarding sensitivity of MPF to patients with MPM, we do not know any other reports.

When two or more tests are available for diagnostic purposes, comparison of the respective AUCs will often show which test is the most effective. ROC curves of MPF yielded an AUC of 0.879, and those of MSLN an AUC of 0.713 (MPF *vs.* MSLN, $p = 0.025$) (Fig. 4A). There was a significant correlation between MPF an MSLN values for MPM (Pearson's correlation coefficient (r_s) = 0.77). This indicates that MPF is probably more sensitive than MSLN for diagnosis of MPM. Though osteopontin and CA125 are also indicated as potential markers in the diagnosis of MPM, neither showed better sensitivity for MPM in comparison with MSLN [20,22].

Physiological cleavage from the mesothelin precursor protein at the furin cleavage site may be responsible for extracellular secretion of MPF [13]. Mesothelin and its variants, attached to cell membranes by GPI-anchors, are also readily released *in vivo*, but the mechanism of mesothelin release has not yet been identified. We transfected the full length of mesothelin variant 1 cDNA into 293 cells and part of mesothelin variant 1 is released from the cell surface and can be measured with the ELISA system (Fig. 2 C, MPF/MSLN-293T). A relevant example is carcinoembryonic antigen (CEA), a tumor-associated GPI-anchored glycoprotein that is commonly shed from the cell surface [23]. The as yet unknown process that mediates a release of the membrane-bound mesothelin variant 1 may be associated with the lower sensitivity of MSLN in comparison with that of MPF. However, additional studies are needed to identify and characterize the process of mesothelin secretion.

Just as MPF and mesothelin originate from the same mesothelin precursor, so adrenomedullin (ADM) and proadrenomedulin (PAMP) are potent vasodilatory peptides derived from a common precursor peptide. However, their short half-life and the presence of a binding protein have been obstacles for an accurate quantification. The ADM precursor is produced in quantities stoichiometric to ADM and PAMP, but is non-functional and stable, while the quantities of the ADM precursor thus produced directly reflect those of ADM and PAMP [24]. One of the reasons for the lower sensitivity of the mesothelin assay could be a lower stability of the protein, but the stability of both proteins needs to be examined and compared.

Pastan's group showed that most ovarian cancer cells express 40-kDa protein mesothelin at the cell surface [25]. MPF was initially isolated from supernatant of pancreatic

cancer cells [26]. Scholler et al. and Hassan et al. independently demonstrated elevated levels of SMRP in 23 of 30 (76.7%) and 40 of 56 (71%) sera from patients with ovarian carcinoma by using a monoclonal antibody, OV569, that was prepared by immunizing mice with ovarian carcinoma cells [10,18]. However, Beyer et al. reported SMRP values were increased in less than 10% of 111 samples collected from ovarian cancer patients [16]. In our study, serum concentrations of both MPF and MSLN were increased in only four of 18 (22.2%) individuals with ovarian cancer. Frequent positive immunostaining for mesothelin is reportedly associated with the non-mucinous type of ovarian cancers [27,28]. Although these reports did not include a description of histological subtype classification in the various blood samples studied, the different ratios of mucinous to non-mucinous type in the samples may partly account for the differences in positivity of serum mesothelin. For MPF, ours is the first reported study of serum levels in ovarian cancer patients.

5. Conclusion

We used ELISA systems developed by us to detect significant differences in the levels of serum MPF and MSLN between MPM patients and controls including lung cancer patients, asbestos-exposed individuals, and normal volunteers. In addition, it is suggested that MPF has superior specificity for MPM compared to MSLN. We are planning a further study to determine the relationship between serum MPF and disease stage, prognosis and histological subtypes.

Conflict of interest

None.

Acknowledgements

The following medical institute and investigator was involved in the study: The First Department of Internal Medicine, Faculty of Medicine, University of Toyama (Ryuji Hayashi).

References

[1] Vogelzang NJ, Rusthoven JJ, Symanowski J, Denham C, Kaukel E, Ruffie P, et al. Phase III study of pemetrexed in combination with cisplatin versus cisplatin alone in patients with malignant pleural mesothelioma. J Clin Oncol 2003;21:2636–44.
[2] Stahel RA. Malignant pleural mesothelioma: a new standard of care. Lung Cancer 2006;54(Suppl 2):S9–14.
[3] Pelucchi C, Malvezzi M, La Vecchia C, Levi F, Decarli A, Negri E. The Mesothelioma epidemic in Western Europe: an update. Br J Cancer 2004;90:1022–4.
[4] Leithner K, Leithner A, Ciar H, Weinhaeusel A, Radl R, Krippl P, et al. Mesothelioma mortality in Europe: impact of asbestos consumption and simian virus 40. Orphanet J Rare Dis 2006;1:44.
[5] Murayama T, Takahashi K, Natori Y, Kurumatani N. Estimation of future mortality from pleural malignant mesothelioma in Japan based on an age-cohort model. Am J Ind Med 2006;49:1–7.
[6] Leigh J, Driscoll T. Malignant mesothelioma in Australia, 1945–2002. Int J Occup Environ Health 2003;9:206–17.
[7] Chang K, Pastan I. Molecular cloning of mesothelin, a differentiation antigen present on mesothelium, mesotheliomas, and ovarian cancers. Proc Natl Acad Sci USA 1996;93:136–40.
[8] Muminova ZE, Strong TV, Shaw DR. Characterization of human mesothelin transcripts in ovarian and pancreatic cancer. BMC Cancer 2004;4:19.
[9] Hellstrom I, Raycraft J, Kanan S, Sardesai NY, Verch T, Yang Y, et al. Mesothelin variant 1 is released from tumor cells as a diagnostic marker. Cancer Epidemiol Biomarkers Prev 2006;15:1014–20.
[10] Scholler N, Fu N, Yang Y, Ye Z, Goodman GE, Hellstrom KE, et al. Soluble member(s) of the mesothelin/megakaryocyte potentiating factor family are detectable in sera from patients with ovarian carcinoma. Proc Natl Acad Sci USA 1999;96:11531–6.
[11] Robinson BW, Creaney J, Lake R, Nowak A, Musk AW, de Klerk N, et al. Mesothelin-family proteins and diagnosis of mesothelioma. Lancet 2003;362:1612–6.
[12] Shiomi K, Miyamoto H, Segawa T, Hagiwara Y, Ota A, Maeda M, et al. Novel ELISA system for detection of N-ERC/mesothelin in the sera of mesothelioma patients. Cancer Sci 2006;97:928–32.
[13] Onda M, Nagata S, Ho M, Bera TK, Hassan R, Alexander RH, et al. Megakaryocyte potentiation factor cleaved from mesothelin precursor is a useful tumor marker in the serum of patients with mesothelioma. Clin Cancer Res 2006;12:4225–31.
[14] Onda M, Willingham M, Nagata S, Bera TK, Beers R, Ho M, et al. New monoclonal antibodies to mesothelin useful for immunohistochemistry, fluorescence-activated cell sorting, Western blotting, and ELISA. Clin Cancer Res 2005;11:5840–6.
[15] Hassan R, Bera T, Pastan I. Mesothelin: a new target for immunotherapy. Clin Cancer Res 2004;10:3937–42.
[16] Beyer HL, Geschwindt RD, Glover CL, Tran L, Hellstrom I, Hellstrom KE, et al. MESOMARK: a potential test for malignant pleural mesothelioma. Clin Chem 2007;53:666–72.
[17] Scherpereel A, Grigoriu B, Conti M, Gey T, Gregoire M, Copin MC, et al. Soluble mesothelin-related peptides in the diagnosis of malignant pleural mesothelioma. Am J Respir Crit Care Med 2006;173:1155–60.
[18] Hassan R, Remaley AT, Sampson ML, Zhang J, Cox DD, Pingpank J, et al. Detection and quantitation of serum mesothelin, a tumor marker for patients with mesothelioma and ovarian cancer. Clin Cancer Res 2006;12:447–53.
[19] Maeda M, Hino O. Molecular tumor markers for asbestos-related mesothelioma: serum diagnostic markers. Pathol Int 2006;56:649–54.
[20] Creaney J, van Bruggen I, Hof M, Segal A, Musk AW, de Klerk N, et al. Combined CA125 and mesothelin levels for the diagnosis of malignant mesothelioma. Chest 2007;132:1239–46.
[21] Cristaudo A, Foddis R, Vivaldi A, Guglielmi G, Dipalma N, Filiberti R, et al. Clinical significance of serum mesothelin in patients with mesothelioma and lung cancer. Clin Cancer Res 2007:5076–81.
[22] Grigoriu BD, Scherpereel A, Devos P, Chahine B, Letourneux M, Lebailly P, et al. Utility of osteopontin and serum mesothelin in malignant pleural mesothelioma diagnosis and prognosis assessment. Clin Cancer Res 2007;13:2928–35.
[23] Khan WN, Hammarstrom S. Biosynthesis of carcinoembryonic antigen (CEA) gene family members expressed in human tumor cell lines: evidence for cleavage of the glycosyl phosphatidyl inositol (GPI) anchor by GPI-PLC and GPI-PLD. Biochem Int 1991;25:723–31.
[24] Ernst A, Hellmich S, Bergmann A. Proneurotensin 1–117, a stable neurotensin precursor fragment identified in human circulation. Peptides 2006;27:1787–93.
[25] Chang K, Pai LH, Batra JK, Pastan I, Willingham MC. Characterization of the antigen (CAK1) recognized by monoclonal

antibody K1 present on ovarian cancers and normal mesothelium. Cancer Res 1992;52:181–6.
[26] Yamaguchi N, Hattori K, Oh-eda M, Kojima T, Imai N, Ochi N. A novel cytokine exhibiting megakaryocyte potentiating activity from a human pancreatic tumor cell line HPC-Y5. J Biol Chem 1994;269:805–8.
[27] Chang K, Pastan I, Willingham MC. Isolation and characterization of a monoclonal antibody, K1, reactive with ovarian cancers and normal mesothelium. Int J Cancer 1992;50: 373–81.
[28] Ordonez NG. Application of mesothelin immunostaining in tumor diagnosis. Am J Surg Pathol 2003;27:1418–28.

Int. J. Cancer: **124,** 1072–1080 (2009)

SRPX2 is overexpressed in gastric cancer and promotes cellular migration and adhesion

Kaoru Tanaka[1,2], Tokuzo Arao[1], Mari Maegawa[1], Kazuko Matsumoto[1], Hiroyasu Kaneda[1,2], Kanae Kudo[1], Yoshihiko Fujita[1], Hideyuki Yokote[1], Kazuyoshi Yanagihara[3], Yasuhide Yamada[4], Isamu Okamoto[2], Kazuhiko Nakagawa[2] and Kazuto Nishio[1]*

[1]*Department of Genome Biology, Kinki University School of Medicine, Osaka-Sayama, Osaka, Japan*
[2]*Department of Medical Oncology, Kinki University School of Medicine, Osaka-Sayama, Osaka, Japan*
[3]*Central Animal Lab, National Cancer Center Research Institute, Chuo-ku, Tokyo, Japan*
[4]*Department of Medical Oncology, National Cancer Center Hospital, Chuo-ku, Tokyo, Japan*

SRPX2 **(Sushi repeat containing protein, X-linked 2) was first identified as a downstream molecule of the *E2A-HLF* fusion gene in t(17;19)-positive leukemia cells and the biological function of this gene remains unknown. We found that *SRPX2* is overexpressed in gastric cancer and the expression and clinical features showed that high mRNA expression levels were observed in patients with unfavorable outcomes using real-time RT-PCR. The cellular distribution of SRPX2 protein showed the secretion of SRPX2 into extracellular regions and its localization in the cytoplasm. The introduction of the *SRPX2* gene into HEK293 cells did not modulate the cellular proliferative activity but did enhance the cellular migration activity, as shown using migration and scratch assays. The conditioned-medium obtained from SRPX2-overexpressing cells increased the cellular migration activity of a gastric cancer cell line, SNU-16. In addition, SRPX2 protein remarkably enhanced the cellular adhesion of SNU-16 and HSC-39 and increased the phosphorylation levels of focal adhesion kinase (FAK), as shown using western blotting, suggesting that SRPX2 enhances cellular migration and adhesion through FAK signaling. In conclusion, the overexpression of SRPX2 enhances cellular migration and adhesion in gastric cancer cells. Here, we report that the biological functions of SRPX2 include cellular migration and adhesion to cancer cells.**

Key words: SRPX2; gastric cancer; cellular adhesion; cellular migration

SRPX2 (Sushi repeat containing protein, X-linked 2) was first identified as *SRPUL* (Sushi repeat protein upregulated in leukemia) by Kurosawa *et al.*[1] The *E2A-HLF* fusion gene causes B-cell precursor acute lymphoblastic leukemia, which is characterized by an unusual paraneoplastic syndrome comprising intravascular coagulation and hypercalcemia; one of the target genes of *E2A-HLF* is *SRPX2*. Apart from the possible involvement of this gene in malignant diseases, a disease-causing mutation (p.N327S) in *SRPX2* resulting in a gain-of-glycosylation aberration in the secreted mutant protein, and the mutation actually leads to rolandic epilepsy with oral and speech dyspraxia and with mental retardation in the French family.[2] While a second mutation (p.Y72S) leads to rolandic epilepsy with bilateral perisylvian polymicrogyria in another family.[3] The involvement of *SRPX2* in these disorders suggests an important role for *SRPX2* in the perisylvian region, which is critical for language and cognitive development.

SRPX2 contains 3 sushi domains and 1 hyaline domain. A sushi domain, also known as a complement control protein module or a short complement-like repeat, contains ~60 amino acids and is found in functionally diverse proteins, such as regulators of the complement activation family, GABA receptor, thyroid peroxidase and selectin family.[4,5] Sushi domains are thought to mediate specific protein–protein or protein–carbohydrate binding and cellular adhesive functions.[4] A phylogenetic analysis revealed that *SRPX2* belongs to a family of 5 genes: *SRPX2*, *SRPX*, *SELP* (selectin P precursor), *SELE* (selectin E precursor) and *SVEP1* (selectin-like protein).[3] *SRPX/SRPX1/EXT1/DRS* has the highest degree of similarity and may be involved in X-linked retinitis pigmentosa.[6,7] The selectin family, which is well known for its biological roles in leukocyte migration, cellular attachment and rolling, also contains sushi domain repeats and are phylogenetic similar to *SRPX2*.[5]

SRPX2 also contains a hyaline (HYR) domain, and this domain probably corresponds to a new superfamily in the immunoglobulin fold. The HYR domains are often associated with sushi domains, and although the function of HYR domains is uncertain, it is thought to be involved in cellular adhesion.[8] Thus, accumulating data on the motifs found in *SRPX2* suggest that *SRPX2* may be involved in cellular adhesion.

We previously performed a microarray analysis of paired clinical samples of gastric cancer and noncancerous lesions obtained from gastric cancer patients[9] and found that *SRPX2* is overexpressed in gastric cancer tissue. The present study sought to clarify the biological function of *SRPX2* expression in gastric cancer.

Material and methods

Cell culture

HEK293 (human embryonic kidney cell line) was maintained in DMEM medium, and SNU-16, HSC-39, 44As3, HSC-43, HSC-44, MKN1 and MKN7 (human gastric cancer cell lines) were maintained in RPMI1640 medium (Sigma, St. Louis, MO) supplemented with 10% FBS (GIBCO BRL, Grand Island, NY). HUVEC (human umbilical vein endothelial cells) was maintained in Humedia-EG2 (KURABO, Tokyo, Japan) medium with 1% FBS under the addition of epidermal growth factor and fibroblast growth factor.

Expression vector construction and viral production

The full-length cDNA fragment encoding human *SRPX2* was obtained from 44As3 cells using RT-PCR and the following primers: SRPX2-F, CGG GAT CCT CAA GGA TGG CCA GTC AGC TAA CTC AAA GAG G; SRPX2-R, CCC AAG CTT GGG CTC GCA TAT GTC CCT TTG CTC CCG ACG CTG GG. The sequences of the PCR-amplified DNAs were confirmed by sequencing after cloning into a pCR-Blunt II-TOPO cloning vector (Invitrogen, Carlsbad, CA). *SRPX2* cDNA was fused to a GFP-containing pcDNA3.1 vector (Clontech, Palo Alt, CA). Empty, GFP and SRPX2-GFP vectors were then transfected into HEK293 cells using FuGENE6 transfection reagent (Roche Diagnostics, Basel, Switzerland). Hygromycin selection (100 μg/mL) was

Grant sponsors: Third-Term Comprehensive 10-Year Strategy for Cancer Control, The Program for the Promotion of Fundamental Studies in Health Sciences of the National Institute of Biomedical Innovation (NiBio), The Japan Health Sciences Foundation.

***Correspondence to:** Department of Genome Biology, Kinki University School of Medicine, 377-2 Ohno-higashi, Osaka-Sayama, Osaka 589-8511, Japan. Fax: +81-72-366-0206. E-mail: knishio@med.kindai.ac.jp

Received 18 June 2008; Accepted after revision 22 September 2008
DOI 10.1002/ijc.24065
Published online 22 October 2008 in Wiley InterScience (www.interscience.wiley.com).